Weierstraß-Institut
für Angewandte Analysis und Stochastik

im Forschungsverbund Berlin e.V.

Preprint ISSN 0946 – 8633

Simulation of Microwave and Semiconductor Laser Structures Including PML: Computation of the Eigen Mode Problem, the Boundary Value Problem, and the Scattering Matrix

Georg Hebermehl[1], Jürgen Schefter[1], Rainer Schlundt[1],

Thorsten Tischler[2], Horst Zscheile[2], Wolfgang Heinrich[2]

submitted: 7th December 2004

[1] Weierstrass-Institute for Applied Analysis and Stochastics
Mohrenstraße 39
10117 Berlin, Germany
E-Mail: hebermehl@wias-berlin.de
schefter@wias-berlin.de
schlundt@wias-berlin.de

[2] Ferdinand-Braun-Institut
für Höchstfrequenztechnik
Gustav-Kirchhoff-Str. 4
12489 Berlin, Germany
E-Mail: tischler@fbh-berlin.de
zscheile@fbh-berlin.de
w.heinrich@ieee.org

No. 987

Berlin 2004

2000 *Mathematics Subject Classification.* 35Q60, 65N22, 65F15, 65F10, 78M25.

Key words and phrases. Microwave device, Semiconductor laser, Simulation, Maxwell's equations, Scattering matrix, Boundary value problem, PML boundary condition, Eigenvalue problem, Linear algebraic equations, Rectangular grids, Tetrahedral nets.

Edited by
Weierstraß-Institut für Angewandte Analysis und Stochastik (WIAS)
Mohrenstraße 39
10117 Berlin
Germany

Fax: + 49 30 2044975
E-Mail: preprint@wias-berlin.de
World Wide Web: http://www.wias-berlin.de/

Abstract

The properties of microwave circuits and optical structures can be described in terms of their scattering matrix which is extracted from the orthogonal decomposition of the electric field. We discretize the Maxwell's equations with orthogonal grids using the Finite Integration Technique (FIT). Maxwellian grid equations are formulated for staggered nonequidistant rectangular grids and for tetrahedral nets with corresponding dual Voronoi cells. The surface of the computation domain is assumed to be an electric or a magnetic wall, open-region problems require uniaxial Perfectly Matched Layer (PML) absorbing boundary conditions. Calculating the excitations at the ports, one obtains eigenvalue problems and then large-scale systems of linear algebraic equations.

Contents

1 Introduction **2**

2 Scattering Matrix **2**

3 Boundary Value Problem **3**

4 Maxwellian Grid Equations **4**

4.1 Staggered Nonequidistant Rectangular Grids 4

4.2 Tetrahedral Grids and Voronoi Cells 4

5 Eigenvalue Problem Including PML **7**

6 Systems of Linear Algebraic Equations Including PML **8**

List of Figures

1 The basic structure under investigation 2

2 Tetrahedron with partial areas of the Voronoi cell faces related to node A 6

1 Introduction

Today, electromagnetic simulation forms an indispensable part in the development of microwave circuits as well as in diode laser design. Since the simulation methods are computationally too expensive to handle complete microwave circuits, analysis has to concentrate on critical parts, such as transmission-line discontinuities and junctions. These elements can be represented by the basic description shown in Fig. 1: a structure of arbitrary geometry which is connected to the remaining circuit by transmission lines. The passive structure (e.g. coplanar waveguide, coupled spiral inductors, via hole, impedance step) forms the central part of the problem. Short transmission line sections are attached to it in order to describe its interaction with other circuit elements.

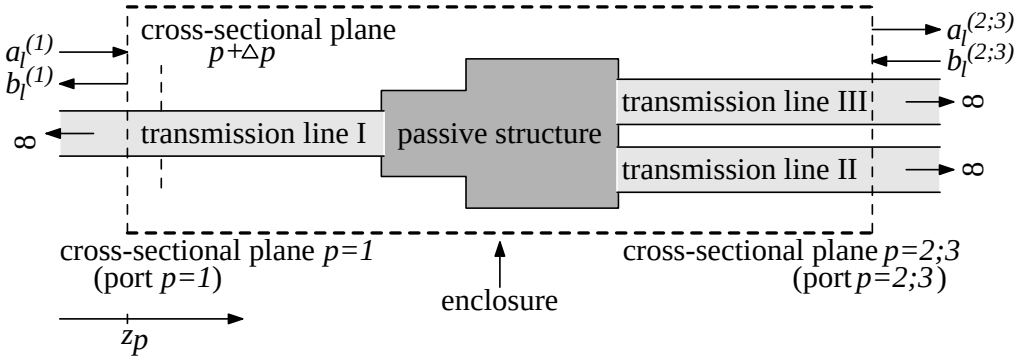

Figure 1: The basic structure under investigation

2 Scattering Matrix

The aim consists in the computation of the scattering matrix, which describes the structure in terms of the wave modes on the transmission line sections at the ports. The wave-mode quantities are derived by assuming the transmission-line sections to be infinitely long and longitudinally homogeneous. The generalized scattering matrix is defined as follows:

$$S = (S_{\rho,\sigma}),\ \ \rho,\sigma = 1(1)m_s, \quad \text{with} \quad m_s = \sum_{p=1}^{\overline{p}} m^{(p)},\ \ \rho = l + \sum_{q=1}^{p-1} m^{(q)}. \qquad (1)$$

$m^{(p)}$ denotes the number of modes which have to be taken into account at the port p. $\overline{p}$ is the number of ports. The modes on a port p are numbered with l, $l = 1(1)m^{(p)}$. That means, the dimension m_s of this matrix is determined by the total number of modes at all ports. The scattering matrix can be extracted from the orthogonal decomposition of the electric field into a sum of mode fields [2]. This has to be done at a pair of neighboring cross-sectional planes z_p and $z_{p+\Delta p}$ on each waveguide for a

number of linearly independent excitations. The electric fields at the planes z_p and $z_{p+\Delta p}$ are calculated solving an eigenvalue problem for the infinitely long waveguide (see section 5) and a boundary value problem for the 3D structure (see section 3), respectively.

The computation of the scattering matrix is based on the orthogonality relation for the electric and magnetic fields of different modes

$$\int_{\Omega} (\vec{E}_{t,l}(z) \times \vec{H}_{t,m}(z)) \cdot d\vec{\Omega} = \eta_m \delta_{l,m}. \tag{2}$$

Here, $\vec{H}_{t,m}$ denotes the transverse magnetic mode fields. In the case of degenerate modes, i.e., the algebraic multiplicity of the corresponding eigenvalues is larger than unity, we have to use first (2) in order to orthogonalize the modes. Details and an example can be found in [5].

3 Boundary Value Problem

A three-dimensional boundary value problem can be formulated using the integral form of Maxwell's equations in the frequency domain [1] in order to compute the electromagnetic field within the structure of interest:

$$\oint_{\partial\Omega} \vec{H} \cdot d\vec{s} = \int_{\Omega} \jmath\omega[\epsilon]\vec{E} \cdot d\vec{\Omega}, \qquad \oint_{\cup\Omega} ([\epsilon]\vec{E}) \cdot d\vec{\Omega} = 0, \tag{3}$$

$$\oint_{\partial\Omega} \vec{E} \cdot d\vec{s} = -\int_{\Omega} \jmath\omega[\mu]\vec{H} \cdot d\vec{\Omega}, \qquad \oint_{\cup\Omega} ([\mu]\vec{H}) \cdot d\vec{\Omega} = 0, \tag{4}$$

$$\vec{D} = [\epsilon]\vec{E}, \;\; \vec{B} = [\mu]\vec{H}, \;\; [\epsilon] = \mathrm{diag}\,(\epsilon_x, \epsilon_y, \epsilon_z)\,, \;\; [\mu] = \mathrm{diag}\,(\mu_x, \mu_y, \mu_z)\,. \tag{5}$$

The electric and magnetic flux densities $\vec{D}$ and $\vec{B}$ are complex functions of the spatial coordinates. $\omega = 2\pi f$ is the angular frequency of the sinusoidal excitation, and $\jmath^2 = -1$. f denotes the frequency.

At the ports p the transverse electric field $\vec{E}_t(z_p)$ is given by superposing weighted transmission line modes $\vec{E}_{t,l}(z_p)$:

$$\vec{E}_t(z_p) = \sum_{l=1}^{m^{(p)}} w_l(z_p)\vec{E}_{t,l}(z_p). \tag{6}$$

The transverse electric mode fields have to be computed solving an eigenvalue problem for the transmission lines (see section 5). All other parts of the surface of the computation domain are assumed to be an electric or a magnetic wall:

$$\vec{E} \times \vec{n} = 0 \quad \text{or} \quad \vec{H} \times \vec{n} = 0. \tag{7}$$

The simulation of open-region problems usually requires absorbing boundary conditions to properly truncate the computational domain. Using the uniaxial Perfectly Matched Layer (PML) absorbing boundary conditions [9] the original form of Maxwell's equations is retained. A complex permittivity $[\epsilon]$ and a complex permeability $[\mu]$ diagonal tensor are introduced, resulting in a reflection-free interface between the computational area and the lossy PML region. On the one hand, the PML allows computing the leakage due to radiation effects, on the other hand, the PML can be used to suppress the influence of the boundary on the electric behavior of the structure.

4 Maxwellian Grid Equations

Maxwellian grid equations are formulated for staggered nonequidistant rectangular grids [1, 12, 7] and for tetrahedral nets with corresponding dual Voronoi cells using the Finite Integration Technique with lowest order integration formulae:

$$\oint_{\partial\Omega} \vec{f} \cdot d\vec{s} \approx \sum(\pm f_i s_i), \quad \int_{\Omega} \vec{f} \cdot d\vec{\Omega} \approx f\Omega. \tag{8}$$

4.1 Staggered Nonequidistant Rectangular Grids

The use of rectangular grids is the standard approach. In general, it is very well adapted to planar microwave structures, since most circuits have a basically rectangular geometry. Using (8) Eqs. (3,4) are transformed into a set of grid equations:

$$A^T D_{s/\mu} \vec{b} = \jmath\omega\epsilon_0\mu_0 D_{A_\epsilon} \vec{e}, \qquad B D_{A_\epsilon} \vec{e} = 0, \tag{9}$$

$$A D_s \vec{e} = -\jmath\omega D_A \vec{b}, \qquad \tilde{B} D_A \vec{b} = 0. \tag{10}$$

The vectors $\vec{e}$ and $\vec{b}$ contain the components of the electric field intensity and the magnetic flux density of the elementary cells, respectively. The diagonal matrices $D_{s/\mu}$, D_{A_ϵ}, D_s, and D_A contain the information on cell dimension and material. A, B, and $\tilde{B}$ are sparse.

By eliminating the components of the magnetic flux density from the two equations on the left-hand sides of (9) and (10), we obtain the system of linear algebraic equations

$$(A^T D_{s/\mu} D_A^{-1} A D_s - k_0^2 D_{A_\epsilon})\vec{e} = 0, \quad k_0 = \omega\sqrt{\epsilon_0\mu_0}, \tag{11}$$

which have to be solved using the boundary conditions (6) and (7), possibly supplemented by PML. k_0 denotes the wavenumber in vacuum.

4.2 Tetrahedral Grids and Voronoi Cells

Using rectangular grids a mesh refinement in one point results in an accumulation of small elementary cells in all coordinate directions, although the refinement is needed

Table 1: Notations

X, Y, Z, W	nodes	l_{XY}	distance of X to Y
XY	edge between X and Y	l^W_{XYZ}	distance of T_{XYZW} to XYZ
XYZ	triangle	d^Z_{XY}	distance of S_{XYZ} to XY
$XYZW$	tetrahedron	a_{XYZ}	area of XYZ
S_{XY}	center of XY	μ_{XYZW}	permeability in $XYZW$
S_{XYZ}	circumcenter of XYZ	ϵ_{XYZW}	permittivity in $XYZW$
T_{XYZW}	circumcenter of $XYZW$		
E_{XY}	magnitude of the electric field on S_{XY}		
B_{XYZ}	magnitude of the magnetic flux density on S_{XYZ}		

only in inner regions. In addition, rectangular grids are not well suited for treatment of curved and non-rectangular structures. A finite-volume method, which uses tetrahedral nets with corresponding Voronoi cells for the three-dimensional boundary value problem, reduces the number of elementary cells by local grid refinement and improves the description of curved structures. The primary grid is formed by tetrahedra and the dual grid by the corresponding Voronoi cells. In this paper, for sake of simplicity, we first assume that the circumcenter of a tetrahedron is located within the tetrahedron. We consider a tetrahedron $ABCD$ with the internal edge AB (see Fig. 2) and the neighbouring elements, which share the edge AB with it. The electric field intensity components are located at the centers of the edges of the tetrahedra, and the magnetic flux density components are normal to the circumcenters of the triangular faces. The Voronoi cells are polytopes. We use the notations given in Table 1 with $X, Y, Z, W \in \{A, B, C, D\}$, where X, Y, Z, W are different from each other, in order to develop the grid equations for tetrahedral nets. E_{XY} and B_{XYZ} satisfy

$$\begin{aligned} E_{XY} &= -E_{YX}, \\ B_{XYZ} &= B_{YZX} = B_{ZXY} = -B_{YXZ} = -B_{XZY} = -B_{ZYX}, \end{aligned} \tag{12}$$

respectively. The PML boundary conditions are not implemented for tetrahedral grids, i.e. one has (see (5)),

$$\mu_x = \mu_y = \mu_z = \mu_{XYZW}, \quad \epsilon_x = \epsilon_y = \epsilon_z = \epsilon_{XYZW}. \tag{13}$$

Using a finite volume approach with the lowest-order integration formulae (8), Eqs. (3) and (4) are transformed into a set of grid equations.

Taking into account the constitutive relations (5) the first equation of (3) is discretized on the dual grid. The internal edge AB is orthogonal to the corresponding Voronoi cell face over which we have to integrate (see Fig. 2). The closed integration path $\partial\Omega$ (see (3) and (8)) consists of the edges with length $s_i = l^W_{XYZ}$, and is the polygon around the periphery of the mentioned Voronoi cell face. The vertices of the polygon are the circumcenters of the tetrahedra which share the edge AB with

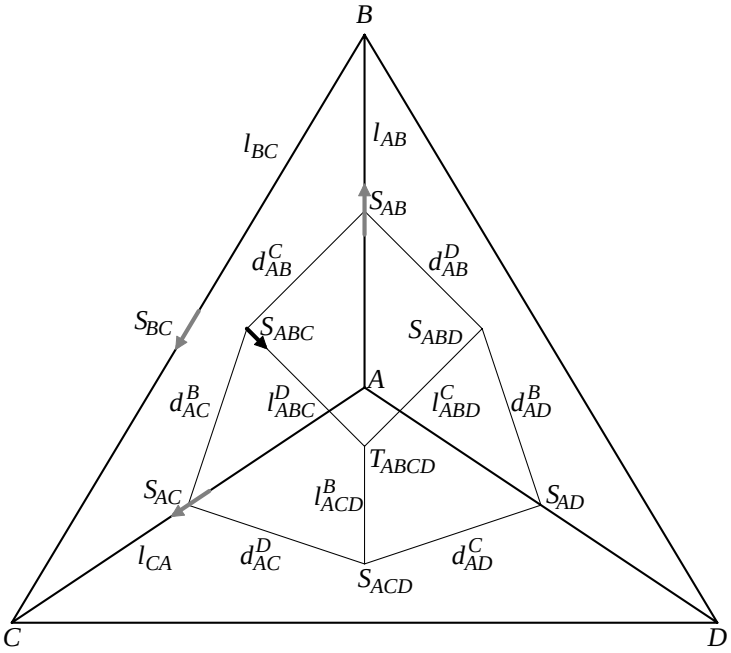

Figure 2: Tetrahedron with partial areas of the Voronoi cell faces related to node A

the tetrahedron $ABCD$. $f_i = B_{XYZ}$ denotes the function values on S_{XYZ}. Ω is the area of the Voronoi cell face. $f = E_{AB}$ denotes the function value on the center S_{AB}. Thus, the discretized equation takes the form:

$$\sum_{CD} \frac{1}{\mu_{ABCD}} \left[l^D_{ABC}\, B_{ABC} + l^C_{ABD}\, B_{ABD} \right] = \jmath\omega \left[\sum_{CD} \frac{1}{2} \epsilon_{ABCD} \left(d^C_{AB}\, l^D_{ABC} + d^D_{AB}\, l^C_{ABD} \right) \right] E_{AB} \tag{14}$$

where the sum is over those tetrahedra $ABCD$ which share the edge AB.

The first equation of (4) is discretized using (8) on the primary grid. We have to integrate over the triangle ABC. This yields the following form:

$$l_{AB}\, E_{AB} + l_{BC}\, E_{BC} + l_{CA}\, E_{CA} = -\jmath\omega a_{ABC}\, B_{ABC}. \tag{15}$$

Now we address the first of the surface integrals (second equation of (3)) reverting to the dual grid. Here, $\cup\Omega$ is a closed surface with an interior volume. The discretization formula (16), with a form similar to the right-hand side of (14) is obtained, except for the additional outer summation taken over all the nodes B neighboring A (in the primary grid). For our final integral equation (second equation of (4)) the primary grid is used again, but now the integration is over the surface of the

tetrahedron $ABCD$. As a consequence, the discretized form (17) can be deduced:

$$\sum_B \left(\left[\sum_{CD} \frac{1}{2} \epsilon_{ABCD} \left(d_{AB}^C \, l_{ABC}^D + d_{AB}^D \, l_{ABD}^C \right) \right] E_{AB} \right) = 0, \tag{16}$$

$$-a_{ABC} \, B_{ABC} - a_{ACD} \, B_{ACD} + a_{ABD} \, B_{ABD} + a_{BCD} \, B_{BCD} = 0. \tag{17}$$

Substituting the components of the magnetic flux density in (14), (15) the number of unknowns in this system can be reduced by a factor of two:

$$\begin{aligned} &\sum_{CD} \frac{1}{\mu_{ABCD}} \left[\left(\frac{l_{ABC}^D}{a_{ABC}} + \frac{l_{ABD}^C}{a_{ABD}} \right) l_{AB} \, E_{AB} + \right. \\ &+ \frac{l_{ABC}^D \, l_{BC}}{a_{ABC}} \, E_{BC} + \frac{l_{ABC}^D \, l_{CA}}{a_{ABC}} \, E_{CA} + \\ &\left. + \frac{l_{ABD}^C \, l_{BD}}{a_{ABD}} \, E_{BD} + \frac{l_{ABD}^C \, l_{DA}}{a_{ABD}} \, E_{DA} \right] = \\ &\qquad \frac{\omega^2}{2} \left[\sum_{CD} \epsilon_{ABCD} \left(d_{AB}^C \, l_{ABC}^D + d_{AB}^D \, l_{ABD}^C \right) \right] E_{AB}. \end{aligned} \tag{18}$$

Here, summation is taken over these tetrahedra $ABCD$, which possess the common edge AB. (18) has to be solved using (12) and the boundary conditions (6) and (7).

5 Eigenvalue Problem Including PML

For the eigenvalue problem, we refer to the rectangular grid [2].

The transverse electric mode fields (see (6)) at the ports of the three-dimensional structure, which is discretized by means of tetrahedral grids, are computed interpolating the results of the rectangular discretization.

The field distribution at the ports is computed assuming longitudinal homogeneity for the transmission line structure. Thus, any field can be expanded into a sum of so-called modal fields which vary exponentially in the longitudinal direction:

$$\vec{E}(x, y, z \pm 2h) = \vec{E}(x, y, z) e^{\mp \jmath k_z 2h}. \tag{19}$$

k_z is the propagation constant. $2h$ is the length of an elementary cell in z-direction. Using ansatz (19) and eliminating the longitudinal electric field components E_z by means of the electric-field divergence equation (see second equation of (3)) we obtain an eigenvalue problem for the transverse electric field $\vec{y}$ on the transmission line region:

$$G\vec{y} = \gamma \vec{y}, \;\; \gamma = e^{-\jmath k_z 2h} + e^{+\jmath k_z 2h} - 2 = -4 \sin^2(h k_z). \tag{20}$$

The sparse matrix G is general complex. The order of G is $n = 2 n_x n_y - n_b$. $n_x n_y$ is the number of elementary cells at the port. The size n_b depends on the number

of cells with perfectly conducting material. The solutions of the eigenvalue problem correspond to the propagation constants of the modes. Using a conformal mapping it can be shown that the eigenvalues corresponding to the few interesting modes of smallest attenuation are located in a region bounded by two parabolas. The modes are found solving a controlled sequence of eigenvalue problems of modified matrices [5] applying the invert mode of the Arnoldi iteration with shifts.

The PML influences the mode spectrum. Modes that are related to the PML boundary can be detected, using a criterion which is based on the comparison between the power concentration inside the PML region to the whole computational domain [11].

This method, developed initially for a reliable calculation of all interesting complex eigenvalues of microwave structures, was expanded then to meet the special requirements of optoelectronic structure calculations. Relatively large cross sections and highest frequencies (i.e., small wavelengths) yield increased dimensions for the eigenvalue problems. Using the results of a coarse grid calculation within the final fine grid reduces the numerical efforts significantly. The use of two levels of parallelization results in an additional speedup in terms of computation time. A laser application can be found in [5].

6 Systems of Linear Algebraic Equations Including PML

All boundary conditions are known after the computation of the eigen mode problem, and the systems of linear algebraic equations can be solved.

Besides the locations and values of the entries, the matrix representations of (14) - (18) have the same structure as (9) - (11). Thus, we refer to (11) for the solution of the linear algebraic equations.

An example, a microwave structure with a microstrip changing its width (impedance step) can be found in [6]. There, for comparison the structure is subdivided in nonequidistant rectangular three-dimensional elementary cells on the one hand and in tetrahedra on the other hand.

Multiplying (11) by $D_s^{1/2}$ yields a symmetric form of linear algebraic equations:

$$\bar{A}\vec{x} = 0, \quad \bar{A} = (D_s^{1/2} A^T D_{s/\tilde{\mu}} D_A^{-1} A D_s^{1/2} - k_0^2 D_{A_{\tilde{\epsilon}}}) \tag{21}$$

with $\vec{x} = D_s^{1/2}\vec{e}$. Moreover, the gradient of the electric field divergence

$$[\epsilon]\nabla([\epsilon]^{-2}\nabla \cdot [\epsilon]\vec{E}) = 0 \tag{22}$$

is used. It can be written as matrix equation

$$\bar{B}\vec{x} = 0, \quad \bar{B} = D_s^{-1/2} D_{A_{\tilde{\epsilon}}} B^T D_{V_{\tilde{\epsilon}\tilde{\epsilon}}}^{-1} B D_{A_{\tilde{\epsilon}}} D_s^{-1/2}. \tag{23}$$

Table 2: Influence of the PML layers on computational efforts.

	Number of Iteration								
	$\omega = 1.00$			$\omega = 1.30$			$\omega = 1.58$		
f/GHz Structure	10	50	100	10	50	100	10	50	100
no PML	63	72	127	51	58	104	45	53	91
z-PML	649	647	716	501	518	591	431	452	543
yz-PML	13 912	27 924	32 298	13 501	29 077	45 371	16 457	44 824	104 642
xyz-PML	12 307	44 723	213 358	11 475	55 221	322 155	15 983	111 965	$> 10^6$
xyz-PML (nonov.)	628	591	742	527	479	609	493	436	624

The diagonal matrix $D_{V_{\hat{e}\hat{e}}}$ is a volume matrix for the 8 partial volumes of the dual elementary cell. In case of tetrahedral grids, the gradient of the divergence at an internal point is obtained considering the partial volumes of the appropriate Voronoi cell.

Taking into account the boundary conditions (6) and (7), Eqs. (21) and (23) yield the form $\hat{A}\vec{x} = \vec{b}$ and $\hat{B}\vec{x} = 0$, respectively, and

$$(\hat{A} + \hat{B})\vec{x} = \vec{b}, \;\; \hat{A} + \hat{B} \text{ complex indefinite symmetric,} \tag{24}$$

can be solved faster than $\hat{A}\vec{x} = \vec{b}$.

Independent set orderings [8], Jacobi and SSOR preconditioning using Eisenstat's trick [3] are applied to accelerate the speed of convergence of the used block Krylov subspace method [4, 10] for the system of linear algebraic equations (24) that has to be solved with the same coefficient matrix, but m_s (see (1)) right-hand sides.

In comparison to the simple lossy case the number of iterations of Krylov subspace methods increases significantly if the structure contains a PML. In this case, among others, the speed of convergence depends on the relations of the edge lengths in an elementary cell of the nonequidistant rectangular. The best results can be obtained using nearly cubic cells. Moreover, overlapping conditions at the corner regions of the computational domain cause an increase of the magnitude of the corresponding off-diagonal elements in comparison to the diagonal of the coefficient matrix. This deteriorates the properties of the matrix. Thus, overlapping PML should be avoided.

The PML layers, which form the absorbing boundary condition, have a significant influence on computational efforts, which is demonstrated in Table 2 for a quasi-TEM waveguide (in Table 2, ω denotes the relaxation parameter of the Krylov subspace method). A nonequidistant mesh of $27 * 24 * 21$ elementary cells including graded PML regions is used, that means the order of the system of linear algebraic equations is 40 824. The structure is symmetric with respect to the (x, z)-plane. Here, a magnetic wall is used, all other parts of the surface are assumed to be

electric walls covered by PML. The longitudinal z-PML region consists of 10 layers, the lateral (x, y)-PML's of 5 layers. The number of iterations also depends on the frequency f and the relaxation parameter ω.

References

[1] Klaus Beilenhoff, Wolfgang Heinrich, and Hans L. Hartnagel. Improved finite-difference formulation in frequency domain for three-dimensional scattering problems. *IEEE Transactions on Microwave Theory and Techniques*, 40, No. 3:540–546, 1992.

[2] Andreas Christ and Hans L. Hartnagel. Three-dimensional finite-difference method for the analysis of microwave-device embedding. *IEEE Transactions on Microwave Theory and Techniques*, 35:688–696, 1987.

[3] S.C. Eisenstat. Efficient implementation of a class of preconditioned conjagate gradient methods. *SIAM J. Statist. Comput.*, 2:1–4, 1981.

[4] R.W. Freund and W. Malhotra. A Block-QMR algorithm for non-Hermitian linear systems with multiple right-hand sides. *Linear Algebra and Its Applications*, 254:119–157, 1997.

[5] Georg Hebermehl, Friedrich-Karl Hübner, Rainer Schlundt, Thorsten Tischler, Horst Zscheile, and Wolfgang Heinrich. Simulation of microwave and semiconductor laser structures including absorbing boundary conditions. *Lecture Notes in Computational Science and Engineering, Springer Verlag*, 35:131–159, 2003.

[6] Georg Hebermehl, Jürgen Schefter, Rainer Schlundt, Thorsten Tischler, Horst Zscheile, and Wolfgang Heinrich. Simulation of microwave circuits and laser structures including PML by means of FIT. *Advances in Radio Science*, 2:107–112, 2004.

[7] Georg Hebermehl, Rainer Schlundt, Horst Zscheile, and Wolfgang Heinrich. Improved numerical methods for the simulation of microwave circuits. *Surveys on Mathematics for Industry*, 9:117–129, 1999.

[8] Y. Saad. Iterative methods for sparse linear systems. *PWS Publishing Company*, 1996.

[9] Z. S. Sacks, D. M. Kingsland, R. Lee, and J.-F. Lee. A perfectly matched anisotropic absorber for use as an absorbing boundary condition. *IEEE Transactions on Antennas and Propagation*, 43:1460–1463, 1995.

[10] Rainer Schlundt, Georg Hebermehl, Friedrich-Karl Hübner, Wolfgang Heinrich, and Horst Zscheile. Iterative solution of systems of linear equations in microwave circuits using a block quasi-minimal residual algorithm. *Lecture Notes in Computational Science and Engineering, Springer Verlag*, 18:325–333, 2001.

[11] Thorsten Tischler and Wolfgang Heinrich. The perfectly matched layer as lateral boundary in finite-difference transmission-line analysis. *IEEE Transactions on Microwave Theory and Techniques*, 48:2249– 2253, 2000.

[12] T. Weiland. A discretization method for the solution of Maxwell's equations for six-component fields. *Electronics and Communication (AEÜ)*, 31:116–120, 1977.